Development of Fast and Easy Methods for Measuring the Young's Modulus of Molding Compounds for IC Packages

Andrej Ivankovic [1], Kris Vanstreels [2], Daniel Vanderstraeten [1], Guy Brizar [1], Renaud Gillon [1], Eddy Blansaer [1] and Bart Vandevelde [2]

[1] ON Semiconductor Belgium
Westerring 15, 9700 Oudenaarde, Belgium
[2] imec, Leuven, Belgium
Kapeldreef 75, 3001 Leuven, Belgium
daniel.vanderstraeten@onsemi.com

Abstract

This work presents two different methods that offer a faster, easier and more straightforward data analysis methods for Young's modulus extraction of plastic molding compound materials. Both methods are compared and verified with the nano-indentation (NI) technique. The originality of this study lies in the fact that the evaluation of these methods focuses not only on Young's modulus extraction from bare molding compound material, but also of molding compounds of packaged IC's as well. The results show also that the NI data analysis is not straightforward due to the inhomogeneous mixture of the different types of materials and fillers inside the molding compound, hence resulting in a complex and rather unknown deformation behavior upon indentation.

1. Introduction

Knowing the Young's modulus is very important for understanding the thermo-mechanical behavior of complex microelectronic devices. This is because Young's modulus has an important impact on the thermo-mechanical stress that is imposed on a packaged IC. Together with the Coefficient of Thermal Expansion (CTE), it determines highly the stresses in the IC package after the packaging processing and during the actual life operation. Therefore, it will impact the lifetime of the product and potential items like warpage, mould cracking, delamination, chip cracking and other package failure problems.

The Young's modulus of plastic molding compounds for device encapsulation, and by this thermo-mechanical stress, is known to be changing over time (due to ageing effects) and under the influence of environmental stresses. For that reason, gaining knowledge on Young's modulus of molding compounds and how it evolves over time and temperature provides valuable information.

Nano-indentation (NI) is a commonly used technique to evaluate the mechanical properties of a huge variety of materials [1, 2]. The advantage of this technique is that it can be used to characterize the mechanical properties of both packaged and bare molding compound materials. However, since a molding compound comprises of a mixture of different type of materials and fillers it puts stringent demands on NI data analysis. Achieving reliable and reproducible data for molding compound material using NI is rather time consuming and certainly not straightforward. Therefore, this paper presents two alternative methods for fast and easy evaluation of Young's modulus of packaged and bare molding compound materials. Both proposed methods are compared and verified with NI results. For this purpose, eight different molding compound types and three different package types were used and aged using high temperature bake. An overview of the different molding compound types used in this work are presented in *table 1*.

Table 1: Overview of the studied molding compound materials measured using the three different techniques

Molding Compound Material	Technique used for Young's modulus extraction		
	Nano Indentation	Bending test	SAM
Material A	X	X	X
Material B		X	X
Material C	X	X	X
Material D		X	X
Material E		X	X
Material F		X	X
Material G	X		
Material H	X		

The first alternative method is based on using a high precision micro-mechanical test system to perform 3-point and 4-point bending tests on beams of bare molding compound. The recorded load-displacement relationship contains information of stiffness of the beams and can be used to extract the Young's modulus by using an easy analytical model. Different loading/unloading rates are chosen to investigate the effect on the extracted values. A reproducibility evaluation of the technique was performed to illustrate the capability of this technique.

The second alternative technique evaluated is scanning acoustic microscopy (SAM). This is a well-known analytical technique used in the IC manufacturing industry for failure analysis of packages (delamination related problems). The standard output of the acoustic microscopy is a two dimensional image but it gives us

also data known as time-of-flight (TOF). This is the time needed for the sound wave to travel through a slab of material. This data can be used to calculate compressional and shear velocities through molding compounds but most importantly their Young's modulus [3, 4]. The evaluation of the SAM technique comprises investigation of the optimal measurement position for molding compound ultrasonic scans on packages including elaboration of specific measurement and parameter extraction problems and a comparison of the results from packaged IC molding compounds versus bare material.

Following techniques are also able to measure the elastic modulus but are not considered in this work: tensile stress strain test on preformed samples, dynamic mechanical analyzer on beams and the impulse excitation technique.

2. Nano-indentation tests

The Young's modulus and hardness of different bare molding compound materials were measured using a nano indenter XP system (MTS Systems Corporation) with a dynamic contact module (DCM) and a continuous-stiffness measurement (CSM) option under constant strain rate condition (figure 1). A standard three-sided pyramid diamond indenter tip (Berkovich) was used for the indentation experiments.

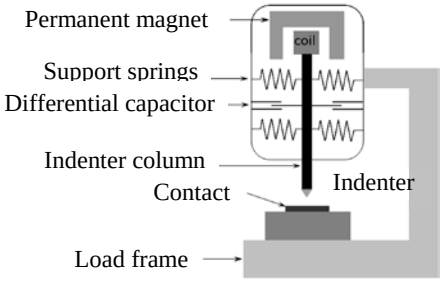

Figure 1 – Schematic illustration of the nano-indentation system, including very sensitive displacement and load sensing systems.

As the indenter tip was pressed into each sample, both depth of penetration (h) and the applied load (P) are monitored. From the collected data, a load-versus-depth curve is then generated. At the maximum indentation depth, the load was kept constant for 10 seconds. During unloading, the tip is withdrawn to 10% of the maximum load and then held in contact with the surface for 60 seconds to correct the recorded data for possible thermal drift. The latter may be caused by local heating of the sample in the vicinity of the indenter tip upon the loading/unloading cycle. From the experimentally obtained load-displacement curve, the Young's modulus (E) and hardness (H) can be calculated based on their relationship to the contact area (A) and the measured contact stiffness (S)

$$S = \beta \frac{2}{\sqrt{\pi}} E_r \sqrt{A} \qquad (1)$$

where E_r is the effective Young's modulus, defined by

$$E_r = \left[\frac{1-\nu^2}{E} + \frac{1-\nu_i^2}{E_i} \right]^{-1} \qquad (2)$$

The latter takes into account the fact that elastic displacements occurred in both the sample, with Young's modulus E and Poisson's ratio ν, and the indenter with elastic constants E_i (1140 GPa) and ν_i (0.07). Using the CSM technique, the contact stiffness, S, can be continuously measured at each indentation depth upon the loading cycle of the indentation tests, hence resulting in a depth profile of the mechanical properties.

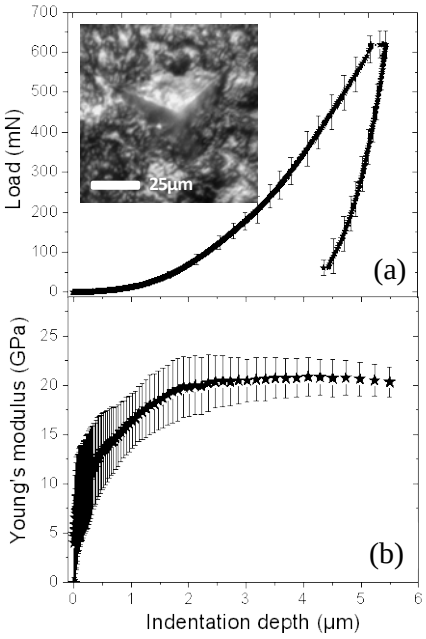

Figure 2 – (a) load-displacement curve of a bare molding compound material (type A and an example of the indent mark). (b) corresponding Young's modulus and hardness depth profile upon loading.

The Poisson's ratio was taken 0.3 for all investigated molding compound materials. *Figure 2* shows the load-displacement curve and corresponding Young's modulus depth profile of 25 independent NI experiments on bare molding compound (type A). Notice that the Young's modulus at indentation depths below 1 µm severely deviates from the bulk values obtained at higher indentation depths. This behavior was observed for all investigated molding compounds and might be attributed to the fact that molding compounds comprise an inhomogeneous mixture of different type of materials and fillers. For indentation depths below 1 µm the contact area between the indenter tip and sample is below 25 µm^2, thereby making it very sensitive to local variations in mechanical properties introduced by the inhomogeneous distribution of filler particles across the sample. At higher indentation depths (above 1µm), the Young's modulus

eventually saturates to the bulk values of the sample because of the increased contact area (about 750 μm^2 at maximum indentation depth). *Table 2* summarizes the Young`s modulus and hardness values for different bare molding compound materials calculated at maximum load. The overall error found in the NI data might be attributed to the sample roughness. This is because the latter can severely influence the point of the first contact between the indenter tip and the sample, which then also influences the calculated contact area and Young's modulus values upon indentation and results in a huge spread on the data.

Table 2 – Estimation for the Young's modulus and hardness of different molding compounds as measured by nano-indentation.

Molding Compound Type	Young's modulus (GPa) at maximum load	Hardness (GPa) at maximum load
A	25,2 ± 2,0	0,79 ± 0,09
C	32,9 ± 5,8	0,98 ± 0,25
G	23,6 ± 3,2	0,75 ± 0,16
H	23,5 ± 1.0	0,92 ± 0,13

3. Bending tests

A high precision micro-mechanical test system from DTS Company (Dauskardt Technical Services) with full computer control and data analysis was used to perform 3-point and 4-point bending tests on bare molding compound beams of fixed dimensions (Length, L=60 mm; Width, B=5 mm; Height, H=1 mm). The system (figure 3) is built around a mechanical stiff frame to improve test stability and yield. It includes an ultra-high-resolution linear actuator providing linear motion of 50 mm with a resolution 20 nm in a compact package. The load cell reads the force and has a maximum load of 220 N. This load can only be applied in the direction axis of the movement. Different loading/unloading rates were chosen, varying between 1 and 25 µm/s.

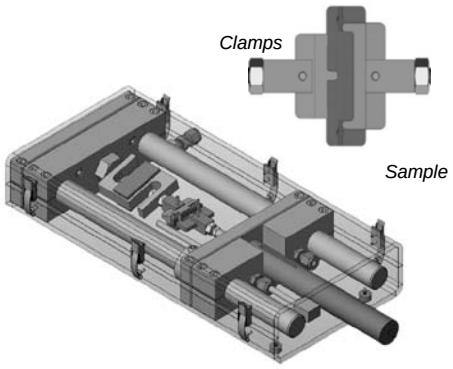

Figure 3 – Schematic drawing of bending test system. The sample is placed between the clamps in either a 3-point or 4-point configuration.

The first bending tests revealed that the experimentally obtained force-displacement curve was independent on the choice of loading/unloading rate. Therefore, in order to increase the speed of execution, the highest loading/unloading rate (25 µm/s) was selected for all subsequent bending tests. The force-displacement curve of beam bending tests contains information on the stiffness of the material under investigation. The initial part of the force-displacement curve is controlled by the local deformation around the supports. Hence, this part is not a straight line, as illustrated on *figure 4a*. When this initial setting is over, the curve is a quasi straight line. The slope of the force-displacement curve allows estimating the Young's modulus of the material. This can be done by comparison between the experimental results and the results of an analytical model.

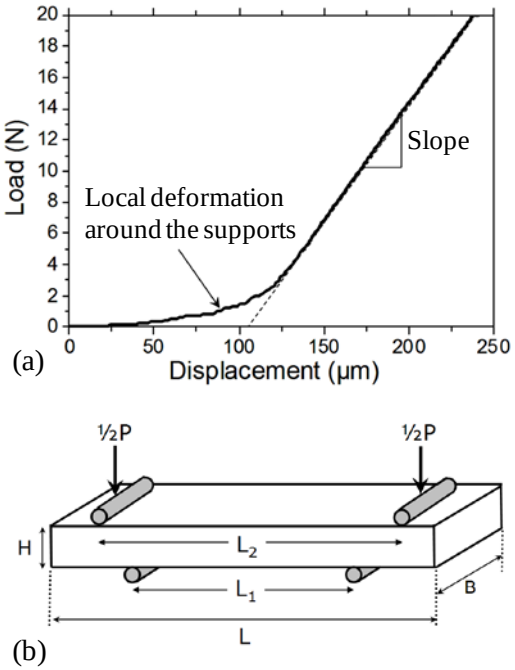

Figure 4 – (a) typical force-displacement curve of bare molding compound using a 4-point bend setup. (b) Schematic of the 4-point bending setup.

In case of a 4-point bending test setup, the slope of the force-displacement relation is related to the Young's modulus (E) of the material and the geometrical parameters of the test sample (B, H) and test configuration (L_1, L_2).

$$P = \left| \frac{B.H^3}{\left[3 \cdot \left(\frac{L_2 - L_1}{2} \right) \cdot \left(\frac{L_1^2 - L_2^2}{4} \right) \right] + \left[\frac{L_2 - L_1}{2} \right]^3} \right| \cdot E \cdot d \qquad (3)$$

where B and H are respectively the width and thickness of the test beams, and L_1 and L_2 are respectively the inner and outer distance between the pins of the 4-point

bending setup (figure 4b) and d and P are the measured displacement and applied force respectively. For rigid materials and small displacements, this equation is also applicable to 3-point bending. *Table 3* compares the Young's modulus values for 6 different bare molding compound beams using 4-point bending and 3-point bending tests. As shown, both beam bending test configurations yield comparable results. Also note that the error bars are much smaller (2-5%) compared to the NI results (5-15%).

Table 3 – estimated Young's modulus of different molding compounds based using 3-point and 4-point bending.

Molding Compound Type	4-point bending (L_1= 50mm; L_2= 22mm)	3-point bending L_1= 40mm
	Young's modulus (GPa)	Young's modulus (GPa)
A	22,9 ± 0,5	23,2 ± 0,4
B	23.1 ± 0,3	23.4 ± 0,4
C	26,6 ± 0,6	26,7 ± 0,5
D	24,6 ± 0,3	24,7 ± 0,4
E	14,4 ± 0,6	15,1 ± 0,5
F	21,7 ± 0,3	21,7 ± 0,4

Figure 5 shows the effect of bake time on the Young's modulus values for 3 different bare molding compound materials using a bake temperature of 175°C. A small increase in Young's was found for all investigated materials. These results also demonstrate the capability of beam bending tests to study the Young's modulus of molding compound materials over time and temperature.

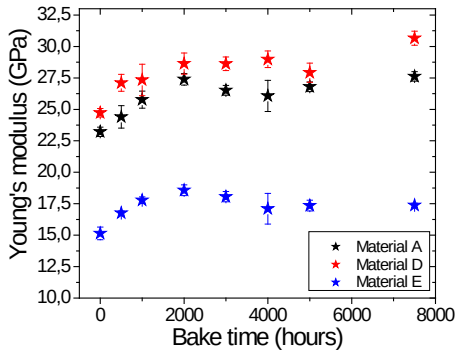

Figure 5: Young's modulus as a function of the bake time at bake temperature 175°C for molding compounds A, D and E.

4. Scanning acoustic microscopy (SAM)

4.1. Introduction to the technique

When attempting to evaluate the capabilities of the SAM for Young's modulus extraction of molding compounds, the main goal was to provide a method which enables simple and low time consuming preparation, device handling, measurements and data analysis. Furthermore, this fast and straightforward process must not undermine the reliability and reproducibility of the acquired data. Clear limitations of the SAM for this purpose were also to be determined. The model used for Young's modulus calculation [3] follows:

$$E = \frac{\rho V_S^2 \left(3V_C^2 - 4V_S^2\right)}{V_C^2 - V_S^2} \tag{4}$$

$$V_C = \frac{2d}{\Delta t_C} \qquad V_S = \frac{2d}{\Delta t_S} \tag{5}$$

$$\nu = \frac{E}{2\mu} - 1 \tag{6}$$

$$\mu = \rho V_s^{\,2} \tag{7}$$

E represents the molding compound's Young's modulus obtained from V_C, the molding compound compressional velocity, V_S, the molding compound shear velocity and ρ, the density of the molding compound. The velocities are equal to the ratio of d, the material thickness and Δt, the time needed for the sound wave to propagate through the material, also referred to as the Time-Of-Flight (*TOF*). μ refers to the shear modulus of the molding compound.

It is important to highlight that due to simplicity the SAM was used only with the compressional transducer (omitting the shear transducer) therefore being utilized solely for obtaining the compressional *TOF* (Δt_c). Consequently, the shear velocity needed in the Young's modulus equation is acquired alternatively by combining equations (4), (6) and (7) resulting in (8):

$$V_S = V_C \sqrt{\frac{3-2(\nu+1)}{4-2(\nu+1)}} \tag{8}$$

From this point onward the compressional *TOF* will be referred to just as *TOF*. Equation (8) now imposes the necessity of importing the Poisson's ratio. In this situation a Poisson's ratio of 0.3 was set for all calculations which in conclusion proved to be a satisfactory balance between simplicity and accuracy with all tested molding compounds. Hereafter, the leftover parameters are the molding compound density (ρ), which can be taken from supplier datasheets, and the material thickness (d). Along with the *TOF*, d is accuracy wise a critical parameter and

should be determined as precise as possible. Additionally, *d* is dependent on the position of the acoustic scan and should be known prior to *TOF* measurement with the SAM.

Two ways of thickness measurement were assessed: utilizing a micrometer tool and with a support of the *Scanning Electron Microscope* (SEM). Although both proved to be precise, with the remark that the SEM can occasionally yield erroneous values due to the scanning angle during operation, the micrometer tool's easy handling and low time consumption imposes itself as a logical choice. During material thickness measurement it is of utmost importance to match the measurement position and the later acoustic scan position as close as possible. This does not strike to be vital in cases with flat equally distant parallel surfaces on each ends, however, warpage and other surface deformations can cause an intake of defective measurement values leading to misleading final results.

In the case of bare molding compound material, received usually in cubical forms, a straightforward approach is enabled with top to bottom measurements. The encapsulated IC's on the other hand are dependent on the optimal acoustic scan position. In this study, three potential scanning positions have been evaluated as shown on *figure 6*:

A) top molding compound surface to top die/silicon surface
B) top molding compound surface to top die paddle surface
C) bottom molding compound surface to bottom die paddle surface

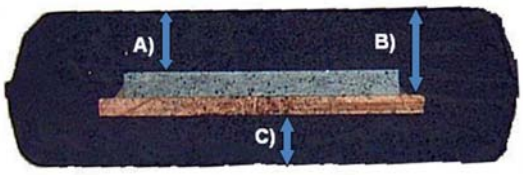

Figure 6: Three potential acoustic scan positions on IC packages

During the evaluation of the Young's modulus extraction from IC packages three different package styles were tested, QFP64, SOM16 and SSOP28, each with different molding compounds. In the case of units in the form of bare mold six different molding compounds were available, as indicated in *table 1* in the introduction.

4.2. Repeatability and reproducibility

Repeatability and reproducibility is an important factor in the data gathering that lead to the Young's modulus extraction of mold compounds. The TOF measurements will require an optimal location for doing the acoustic scans but also the selection of the optimal measurement conditions and therefore directly ensuring repeatability and reproducibility.

The scans were carried out on 7 units of each package style and on all positions presented in *figure 6.* To ensure equal scanning conditions, all of these units were placed together in the water tank of the acoustic microscope as shown on the 2D SAM image in *figure 7. Figure 8* depicts a sample scan of the SAM measured *TOF* from the molding compound top to the die paddle top. The blue graph (longer *TOF*) represents the reflected sound wave pulses from a virgin unit, while the red graph (shorter *TOF*) represents the reflected sound wave pulses from the same unit after temperature storage at 27°C for 168h. Both graphs prove a stable *TOF* and moreover, a change in its value due to effects of heat on the molding compound. Additionaly, the stressed unit shows an inverted sound wave pulse reflected from the die paddle top compared to the virgin unit pulse.

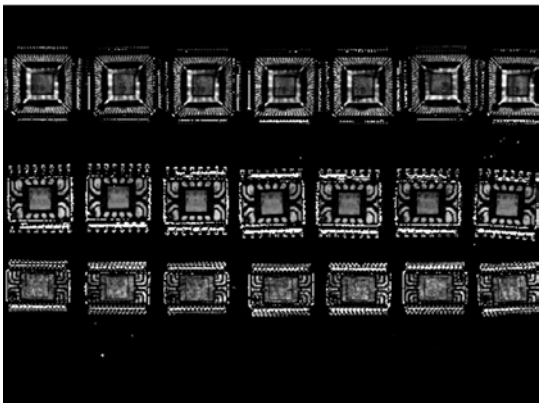

Figure 7: 2D SAM image of packages during SAM measurements

This inverted signal points out the additional influence on *TOF* shifts due to delamination induced signal path reduction consequently resulting in misleading *TOF* values. This is the main reason for dismissing acoustic scans on stressed units from the top side to the die paddle top or die top. Although, this scanning position can be utilized if a repeatable position with no delamination can be found on units after stress tests.

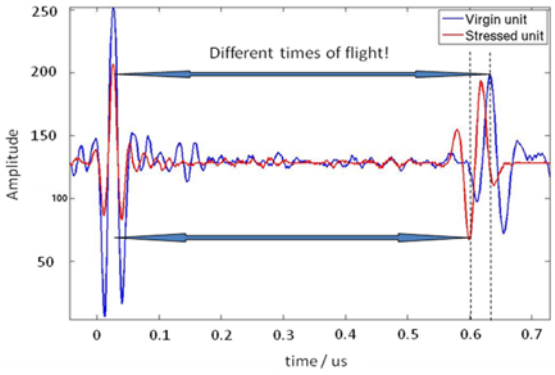

Figure 8: Reflected acoustic signal from the molding compound top and die paddle top

The preferred position for acoustic scans on molding compounds on packages resulting from this evaluation is from the outer package bottom side to the die paddle bottom, indicated with the letter C on *figure 6*. This position was found to give the most stable and accurate results in addition to minimizing the delamination influence risk.

Figure 9 shows the assuring Young's modulus repeatability results for 7 virgin units of the SOM16 package style taken from the back side. Measurements were done three times after each other by repeatedly drying and inserting the packages again in the SAM water tank. To verify and confirm the choice of the package back side as the optimal acoustic scan position the standard deviation of Young's modulus values from SAM measurements on the package setup presented on *figure 7* were calculated. *Figure 10* clearly shows that on all 3 package styles the lowest standard deviation comes from scanning position C, being the package bottom side molding compound surface to the die paddle bottom.

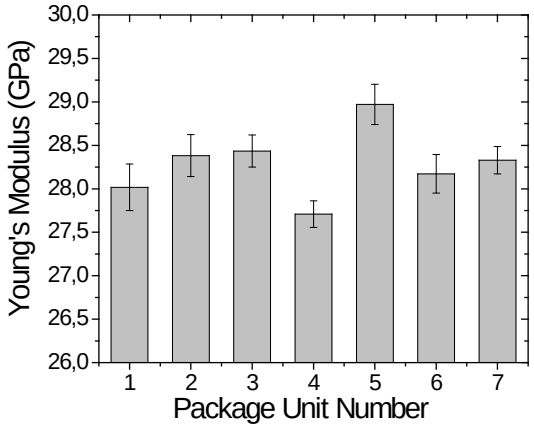

Figure 9: Repeatibility of Young's modulus values with acoustic scans from the back package side

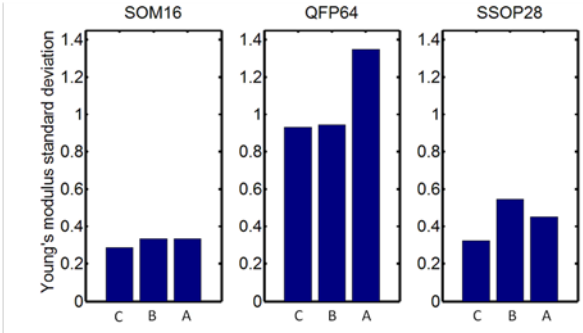

Figure 10 –Young's modulus standard deviation by package style and acoustic scan position

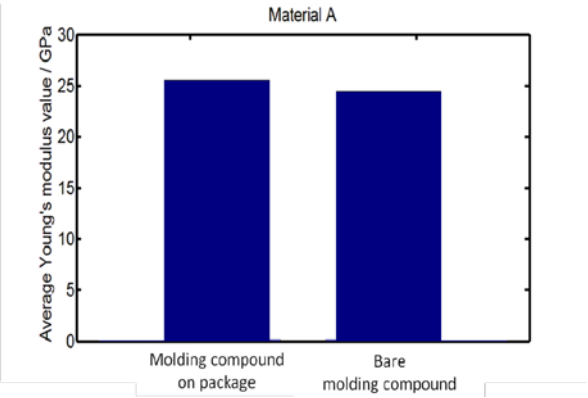

Figure 11 – Average Young's modulus comparison of material A on packages and in bare mold form

A final comparison was made by averaging Young's modulus results from the same material obtained from 7 bare mold units and 7 IC encapsulants, taken from the back side. The results, presented on *figure 11*, show that the two Young's modulus values are in line therefore supporting the SAM extracted Young's modulus as a fast and successful technique.

4.3. SAM measurement precautions

In order to prevent *TOF* extraction related problems during the acoustic measurements, care should be taken of the following: the water used in the SAM tank in which the units are placed should be always clean. This encompasses contamination in the form of dust or other particles and intruding grease. Furthermore, the units to be measured should be placed on a flat, prefferably glass surface, temporarily sticked to this backgound by attaching material to prevent movement. In addition to these precautions, the reflected acoustic signals should be gathered from brighter areas seen on the the 2D SAM monochrome image due to higher signal amplitude values in those positions.

5. Comparison of methods

Figure 12 compares the Young's modulus values of 2 different types of mold compound materials (type A and C) extracted with 3 different techniques (SAM, bending tests and NI). As can be extrapolated from the graphs, a very good agreement is found between the bending tests and SAM measurements. The reproducibility of both methods is good and the error on the extracted Young's modulus values is much smaller than compared to the NI technique.

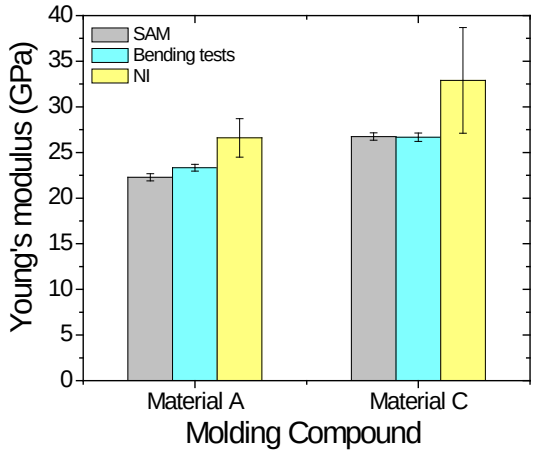

Figure 12: comparison of Young's modulus values for two different mold compound types using 3 different techniques.

Table 4 compares the three techniques with respect to the application of the technique (packaged/non packaged samples), the measurement time that is needed to perform reliable, reproducible results and data analysis. The main advantage of NI on mold compound materials is that it can be used to characterize the mechanical properties of both packaged and bare molding compound materials. The disadvantage of this technique is the time consuming and not straightforward data analysis. Bending tests on the other hand, offer a fast and easy way to determine the Young's modulus of molding compounds.

Table 4: Comparison of different techniques for Young's modulus extraction

Technique	Application		Measurement time	Data analysis
	Packaged molding compound	Bare molding compound		
Nano indentation	☺	☺	☹	☹
Bending tests	☹	☺	☺	☺
SAM	☺	☺	☺	☺

However, this technique can only be applied to bare molding compound materials. The best results were obtained with the SAM technique, which not only provides easy and fast extraction of Young's modulus on both packaged and bare molding compound materials, but also in a non-destructive way.

6. Conclusions

The most important potential impact of this study is that we can demonstrate easy and fast measurement methods for Young's modulus extraction valid not only for bare molding compound materials, but also for molding compounds on already packaged units as well.

It was shown that the three measurement techniques considered in this work give similar results. Each of the techniques have there advantages and limitations, and therefore, the technique which will be used, is function of sample construction, the required measurement time and the number of measurements to have good statistics. Some of the techniques can give also additional information, e.g. the bending experiment can give yield stress and ultimate strength while the nano-indentor gives hardness information.

Acknowledgments

The authors would like to acknowledge the support, logistics and input from ON Semiconductor and IMEC researchers. The authors also would like to thank the support by MEDEA+ and IWT for funding the ELIAS project.

References

1. Oliver W. C., and Pharr G. M., "An improved technique for determining hardness and elastic modulus using load and displacement sensing indentation experiments", J. Mater. Res. 7 (3), pp. 613 (1992).
2. Fischer-Cripps, A. C., Nanoindentation, 2nd ed. (Springer: New York, 2004), pp. 69-110, 132-143.
3. Canumalla, S., Oravecz, M.G., "Nondestructive Elastic Property Characterization of IC Encapsulants", *Applications of Fracture Mechanics in Electronic Packaging*, ASME IMECE (1997)
4. Clement, A., Saint-Paul, M., "Ultrasonic measurements of microelectronic molding compounds", *Journal of Materials Science: Materials in Electronics 13* (2002), pp. 21-25.